

Article

# Increasing Weekend Effect in Ground-Level O<sub>3</sub> in Metropolitan Areas of Mexico during 1988–2016

Iván Y. Hernández-Paniagua <sup>1</sup>, Rodrigo Lopez-Farias <sup>1</sup>, José J. Piña-Mondragón <sup>1</sup> ,  
Juan A. Pichardo-Corpus <sup>1</sup> , Olivia Delgadillo-Ruiz <sup>1</sup> , Arnoldo Flores-Torres <sup>1</sup>,  
Agustín García-Reynoso <sup>2</sup> , Luis G. Ruiz-Suárez <sup>2</sup>  and Alberto Mendoza <sup>3,\*</sup> 

<sup>1</sup> CONACYT—Consortio CENTROMET, Camino a Los Olvera 44, Los Olvera, Corregidora 76904, Querétaro, Mexico; iyassmany@hotmail.com (I.Y.H.-P.); rodrigo.lopez@centromet.mx (R.L.-F.); joaquin.pina@centromet.mx (J.J.P.-M.); juan.pichardo@centromet.mx (J.A.P.-C.); olivia.delgadillo@centromet.mx (O.D.-R.); arnoldo.flores@centromet.mx (A.F.-T.)

<sup>2</sup> Centro de Ciencias de la Atmosfera, Universidad Nacional Autónoma de México, Circuito de la Investigación Científica S/N, Ciudad Universitaria, Coyoacán, Ciudad de México 04510, Mexico; agustin@atmosfera.unam.mx (A.G.-R.); ruizsu@unam.mx (L.G.R.-S.)

<sup>3</sup> Escuela de Ingeniería y Ciencias, Tecnológico de Monterrey, Av. Eugenio Garza Sada 2501, Monterrey 64849, Nuevo León, Mexico

\* Correspondence: mendoza.alberto@itesm.mx; Tel.: +52-81-8158-2091

Received: 28 August 2018; Accepted: 10 September 2018; Published: 18 September 2018



**Abstract:** Here, we present an assessment of long-term trends in the O<sub>3</sub> weekend effect (WE) occurrences and spread within the Mexico City (MCMA), Guadalajara (GMA), and Monterrey (MMA) metropolitan areas, which are the three largest metropolitan areas (MAs) of Mexico and concentrate around 33% of the total population in the country. Daytime averages and peak differences in O<sub>3</sub> concentrations from weekdays to weekends were used as a proxy of WE occurrence. All MAs exhibited the occurrence of WE in all years at least in one monitoring site. Substantial differences in O<sub>3</sub> daytime averages and peaks from weekdays to weekends have decreased over time in all MAs, and since 1998 and 2013 for the MCMA and GMA, respectively, higher O<sub>3</sub> levels during weekends are typical during most of the year. The largest variations in the O<sub>3</sub> WE were observed at downwind and urban core sites of the MCMA and GMA. Significant increasing trends ( $p < 0.05$ ) in the O<sub>3</sub> WE magnitude were observed for Sundays at all sites within the MCMA, with trends in annual averages ranging between 0.33 and 1.29 ppb O<sub>3</sub> yr<sup>-1</sup>. Within the GMA, for Sundays, fewer sites exhibited increasing trends in the WE occurrence and at lower growth rates (0.32 and 0.48 ppb yr<sup>-1</sup>,  $p < 0.1$ ) than within the MCMA, while within the MMA no apparent trends were observed in marked contrast with the MCMA and GMA. Our findings suggest that policies implemented have been successful in controlling weekday ground-level O<sub>3</sub> within the MCMA and GMA, but further actions must be introduced to control the increases in the O<sub>3</sub> WE magnitude and spread.

**Keywords:** long-term trends; O<sub>3</sub> precursor emissions; policy; surface O<sub>3</sub>; spatiotemporal trends

## 1. Introduction

Tropospheric O<sub>3</sub> is a secondary air pollutant formed by photo-oxidation of volatile organic compounds (VOCs), carbon monoxide (CO), and methane (CH<sub>4</sub>) in the presence of nitrogen oxides (NO<sub>x</sub> = NO + NO<sub>2</sub>). It may cause deleterious effects on human health and vegetation [1,2], and act as an effective greenhouse gas [3,4]. In large metropolitan areas, high levels of tropospheric O<sub>3</sub> are typical during seasons with intense photo-chemical processing and stable high-pressure systems that prevent dispersion of precursor emissions. In metropolitan areas of US and Canada, VOC and NO<sub>x</sub> emissions

have decreased significantly during the last two decades in response to the introduction of stricter emission standards for motor vehicles and industries, which has helped to improve the air quality [5–7]. Nevertheless, strong weekly patterns with lower emissions of NO<sub>x</sub> and VOCs during weekends than on weekdays have resulted in the so-called “O<sub>3</sub> weekday/weekend effect” (WE) [8], which is the occurrence of higher concentrations in ground-level O<sub>3</sub> during weekends than during weekdays.

The O<sub>3</sub> WE is explained by non-linearity of the system of O<sub>3</sub> production, which may lead to increases in production rates of O<sub>3</sub> with increasing NO<sub>x</sub>, whereas for other conditions the production rates may decrease with increases in NO<sub>x</sub> and/or VOCs [1]. Such behaviour complicates the effective design and implementation of control strategies for reducing ground-level O<sub>3</sub>, and highlights the need for conducting periodic evaluations of the results achieved by existing policies. This phenomenon was reported first in the 1970s in the New York–New Jersey region [9] and Baltimore–Washington metropolitan areas [10], and at the Los Angeles basin [11]. Nevertheless, only recently, the combination of the modelling approach, continuous monitoring and field studies has shown the complexity of this phenomenon associated with local meteorology, physiography, and changes in precursor emissions [12]. Thus, ground-level O<sub>3</sub> during weekends over time may increase, decrease, or not vary in relation to weekdays from city to city [12,13]. In urban areas with significant O<sub>3</sub> precursors emissions from motor vehicles, decreases during weekends of up to 50% and 20% in NO<sub>x</sub> and VOC emissions, respectively, may result typically in changes of around ±10% in ground-level O<sub>3</sub> [14,15].

In the US, a national analysis of weekday/weekend differences in O<sub>3</sub> from 1997–1999 to 2008–2010 shown the vanishing of higher concentrations during weekends than weekdays, from around 35% to less than 5% of the sites studied in response to a greater decline in NO<sub>x</sub> emissions [12]. By contrast, for the Santiago metropolitan area in Chile, Seguel et al. reported a significant increase since 2004 in diurnal average concentrations in ground-level O<sub>3</sub> during weekends than during weekdays [16]. Such increase was associated with an increase in the VOC/NO<sub>x</sub> ambient ratio due to lower NO<sub>x</sub> emissions from motor vehicles during weekends. In the Mexico City metropolitan area (MCMA), non-significant changes during 2001–2007 in ground-level O<sub>3</sub> from weekdays to Saturday and Sunday were reported by Stephens et al. with only occasional higher O<sub>3</sub> concentrations during weekends despite relatively lower emissions of precursors [17]. The little change in O<sub>3</sub> from weekdays to weekends was attributed to workday O<sub>3</sub> production being limited by VOCs and inhibited by NO<sub>x</sub> and, small or no changes in the VOC/NO<sub>x</sub> ratio due to simultaneous decreases in VOCs and NO<sub>x</sub> emissions during weekends.

Ground-level O<sub>3</sub> in the MCMA has decreased constantly since the 1990s in response to several primary pollutant emissions reduction initiatives [18–20]. By contrast, O<sub>3</sub> levels in the Guadalajara metropolitan area (GMA) and Monterrey metropolitan area (MMA), the second and third largest cities in the country, respectively, have remained constant or increased during the same period due to the relatively little attention to control precursor emissions [21]. Nevertheless, O<sub>3</sub> pollution episodes are still observed in the MCMA to date. For instance, during March 2016, a high-pressure system caused high O<sub>3</sub> concentrations up to 185 ppb. To reduce such high levels, emergency actions implemented included the driving restriction to around 40% of the overall vehicular fleet and, industrial and service cuts, which apparently worsened the event and have been maintained ever since [22]. Additional actions such as the driving restriction on Saturdays for vehicles with plate registration out of the MCMA have contributed also to decrease emissions during weekends, modifying the O<sub>3</sub> production system. The observed decrease in ground-level O<sub>3</sub> within the MCMA has resulted in lower violations to the national official standard (NOM-020-SSA1-2014), which currently sets the maximum permitted level in 95 ppb O<sub>3</sub> as a 1 h average. Therefore, it is imperative to examine the results from the MCMA O<sub>3</sub> precursor control emissions policies implemented in order to better understand the atmospheric chemistry and to identify the policies to be applied in other metropolitan areas in Mexico.

Existing studies have addressed the O<sub>3</sub> weekend effect within the MCMA [17,23] and O<sub>3</sub> sensitivity for the Monterrey Metropolitan Area (MMA) [24]. However, none of those has considered

changes in the WE of ground-level O<sub>3</sub> in metropolitan areas of Mexico. In this study, we describe trends in the WE occurrence and magnitude within the three major metropolitan areas of Mexico. Long-term and high-frequency measurements of O<sub>3</sub> recorded at five air quality stations within the MCMA, Guadalajara (GMA), and MMA were used to assess changes in emission precursors from weekdays to weekends since the 1990s. In order to better assess temporal and spatial changes in the WE from year to year, a time window for the peak occurrence in O<sub>3</sub> was defined using an exploratory analysis of the collected data sets. Finally, we describe how decreasing trends in O<sub>3</sub> precursor emissions have resulted in lower O<sub>3</sub> levels during weekdays but led to higher levels on weekends.

## 2. Methodology

### 2.1. Metropolitan Areas Description

The MCMA is located in Central Mexico (19°22' N, 99°09' W) and has a surface area of around 9500 km<sup>2</sup> (Figure 1). It lies at an average altitude of 2500 m a.s.l. and is surrounded completely by mountains. The MCMA has a population of around 20.1 million inhabitants, which makes it the most populous city in Mexico [25]. The climate is mild with an annual average temperature of 17.5 °C and an annual average rainfall of 846 mm. The predominant wind direction throughout the year at the MCMA (Figure 1). It has the largest vehicle fleet in the country with around 8.9 million motor vehicles and a motorization index of 0.4. In the MCMA, air pollutants emitted primarily from the industrial, transport, and service sectors have led to poor air quality compared with other large cities in Mexico and with other megacities worldwide [26,27].

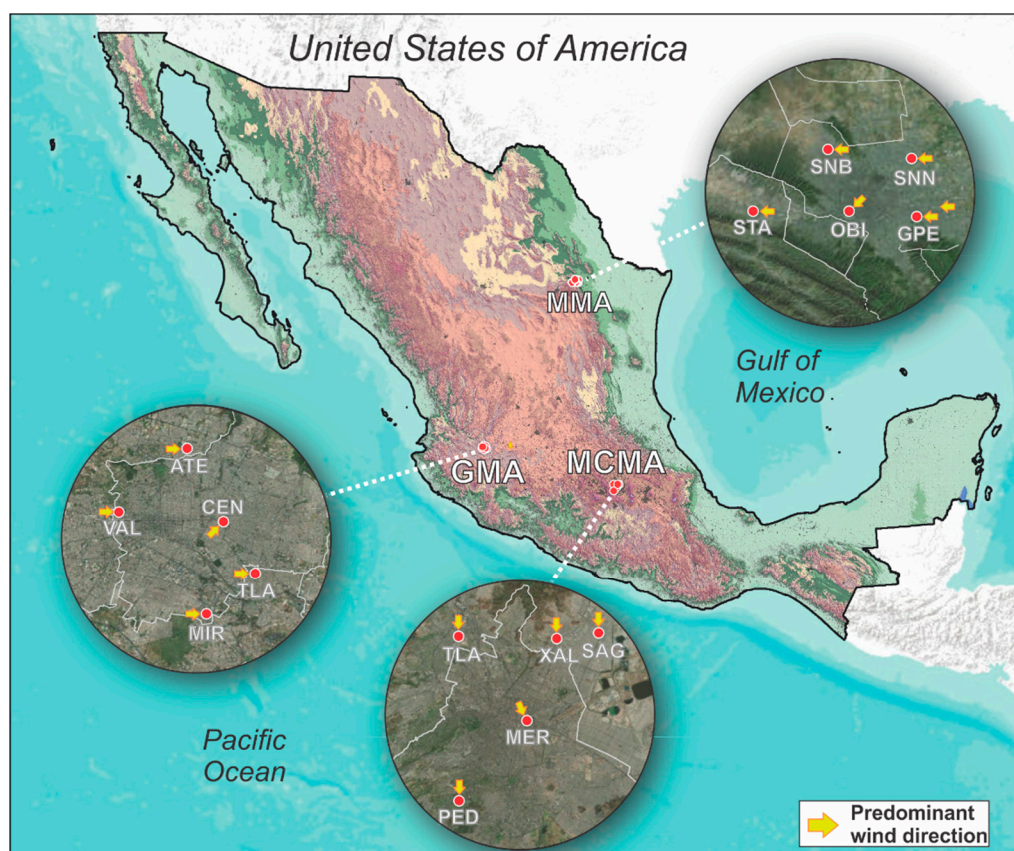


**Figure 1.** The Mexico City (MCMA), Guadalajara (GMA), and Monterrey (MMA) metropolitan areas in the national context and the monitoring sites in relation to each metropolitan area. The red arrows show the predominant wind direction at each site throughout the year.

The GMA is located NW of MCMA (20°40' N, 103°21' W; Figure 1), covers an area of 3600 km<sup>2</sup> and lies at an average altitude of 1550 m a.s.l. It has around 4.9 million inhabitants, which makes it the second most populous urban area in Mexico [25]. The climate is mild with dry springs and wet summers. The annual average temperature is 19.3 °C, and the annual average rainfall is 868 mm. Westerly winds dominate at the GMA during most of the year (Figure 1). The vehicle fleet is comprised of around 2.1 million motor vehicles, with a motorization index of 0.4. The GMA experiences occasional pollution events during stagnation events due to local emissions from automobiles, industry and commercial and services activities [28].

The MMA is located north of the MCMA, around 200 km south of the US border (25°40' N, 100°20' W; Figure 1). It lies at an average altitude of 550 m a.s.l. and is surrounded by mountains to the south and west. It has a population of around 4.2 million, which makes it the third most populous urban area in the country [25]. The climate is semi-arid with an annual average rainfall of 590 mm, and an annual average temperature of 25.0 °C with hot summers and mild winters. At the MMA, the predominant wind direction is east during most of the year (Figure 1). It has a vehicle fleet of around 1.9 million motor vehicles and a motorization index of 0.4. In the MMA, rapid weather changes and enhanced industrial activity may cause recurrent pollution events during spring and winter [21].

## 2.2. O<sub>3</sub> Measurements, Instrumentation, and Calibration

In order to protect the population health in metropolitan areas of Mexico, the environmental legislation makes compulsory the continuous monitoring of ground-level O<sub>3</sub> and five additional air pollutants (CO, NO<sub>2</sub>, SO<sub>2</sub>, PM<sub>10</sub>, and PM<sub>2.5</sub>), along with seven meteorological parameters (wind speed (WS), wind direction (WD), temperature (Temp), rainfall, solar radiation (SR), relative humidity (RH), and pressure). In all MAs, ground-level O<sub>3</sub> is measured, in accordance with EPA EQOA-0880-047, using Thermo Environmental Instruments Inc. (TEI) model 49 UV photometric analysers with a stated precision of less than ±2 ppb O<sub>3</sub> and a detection limit of 2 ppb O<sub>3</sub>. The continuous records are summarized as hourly averages and stored in the official air quality department websites of each metropolitan area. Hourly O<sub>3</sub> data, valid with a minimum data capture of 75%, were downloaded from the Atmospheric Monitoring System (SIMAT) of the MCMA (<http://www.aire.cdmx.gob.mx>), from the Atmospheric Monitoring System (SIMAJ) of the GMA (<http://siga.jalisco.gob.mx/aire/>), and from the Integral Environmental Monitoring System (SIMA) of the MMA (<http://aire.nl.gob.mx/>). We used data recorded at monitoring sites representative of different environments within the three MAs, which are not directly influenced by strong emission sources [29].

Measurements, calibration, maintenance procedures, and quality assurance/quality control (QA/QC) followed the protocols established in the Mexican standards NOM-036-SEMARNAT-1993 and NOM-156-SEMARNAT-2012. All data sets have been validated by the Air Quality Research Division of the Environment and Natural Resources Secretariat (SEMARNAT). All data validation protocols follow standards established by the US Environmental Protection Agency [30]. Further details of the MCMA, GMA, and MMA O<sub>3</sub> records can be found elsewhere [20,21].

## 2.3. Calculation of the Weekend Effect (WE)

To assess temporal changes in ground-level O<sub>3</sub> from weekdays to weekends during the studied periods, we used two metrics reported in the literature [31] and references therein. First, we calculated differences in O<sub>3</sub> daytime averages (06:00–18:00 CDT) by subtracting the average concentrations from Tuesday to Thursday from the Saturday and Sunday average, as:

$$WE_{AVG}(\text{WEEK}, \text{WEEKEND}) = \text{AVG}(\text{WEEKEND}) - \text{AVG}(\text{WEEK}) \quad (1)$$

where WEEK = {D<sub>TUE</sub>, D<sub>WED</sub>, D<sub>THU</sub>} and WEEKEND = {D<sub>SAT</sub>, D<sub>SUN</sub>} are a set of O<sub>3</sub> concentrations from weekday and weekend reference days, and AVG is the O<sub>3</sub> concentration averaged from each O<sub>3</sub>

set. Thus,  $WE_{AVG}$  is the difference between daytime  $O_3$  from Saturday to Sunday minus Tuesday to Thursday (Sat–Sun/Tue–Thu).

Second, we calculated differences in  $O_3$  highest concentrations (peaks) between reference days within the same week, e.g., weekend (Saturday, Sunday) minus weekday (Wednesday), as:

$$WE(D_{NWN}, D_{NWD}) = \text{MAX}(D_{NWN}) - \text{MAX}(D_{NWD}) \quad (2)$$

where  $WE$  is the difference calculated by subtracting the highest value observed on Wednesday ( $D_{NWD}$ ) from the highest value observed on Saturday (Sat/Wed) or Sunday (Sun/Wed) ( $D_{NWN}$ ).  $D_{NWD}$  and  $D_{NWN}$  are vectors expressed in concentration (ppb  $O_3$ ) from the same week with  $n$  missing data in the reference days.  $NWN \in \{\text{Sat, Sun}\}$  and  $NWD \in \{\text{Tue, Wed, Thu}\}$  are indexes with values from a given week. Thus, if  $WE(D_{NWN}, D_{NWD}) > 0$ , a  $WE$  is detected; otherwise, there is no  $WE$ .

To discard bias in the  $WE$  calculation due to missing data, the  $O_3$  time-series were filtered for retaining only reference days with no missing values during the peak occurrence maximum probability time window. The time window was defined from a peak probability distribution for each monitoring site, calculated from days with no missing values, e.g., 24 values per day. Then, the  $O_3$  peak timing was determined from the filtered data set for each metropolitan area and site. Finally, the overall peak probability distribution was constructed from the whole data sets with no missing values during the  $O_3$  peak timing established from the filtered data set. A 50% data capture threshold was used in order to consider the  $WE$  calculation valid. Figure 2 shows the overall peak probability distributions for each monitoring site and metropolitan area, and Table S1 shows the recovered data by monitoring site for the  $WE$  calculation.

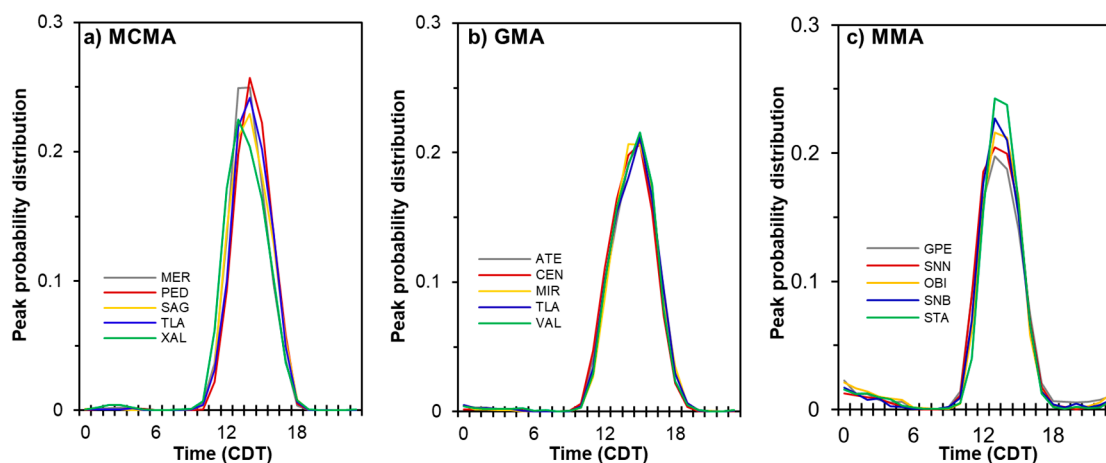


**Figure 2.** Peak probability distributions by monitoring site calculated from the filtered data sets for the (a) MCMA; (b) GMA and (c) MMA.

#### 2.4. Spatial Interaction Calculation

To show the  $WE$  spatial extent at each metropolitan area, we assessed the  $WE$  spatial interaction among sites per year. The  $WE$  spatial interactions were assessed using the graph theory approach [32], which allows the analysis of interactions among monitoring sites over time. We represent the  $O_3$  annual averages calculated from differences in  $O_3$  peaks in a vector  $D$ ; thus, we have a sequence of vectors  $D_i$  with  $i \in \{1, 2, \dots, n\}$ , where  $n$  is the number of years with  $WE$  data for each metropolitan area. The length of each  $D_i$  is 5, as it corresponds to the number of sites selected for a better spatial representation. We used the vectors  $D_i$  to build a graph (network) by year with the set of vertices (nodes) representing sites and edges (links), which allows measuring the relation from site to site. A summary of graph theory notation is presented for a better interpretation of the calculation steps. Briefly, a graph  $G = (V, E)$  consists of a set  $V$  of vertices and a set  $E$  of edges.  $n(G) = |V|$  is the number of vertices of  $G$ , and  $m(G) = |E|$  is the number of edges, henceforth referred as  $n$  and  $m$ , respectively.

A graph  $H = (V_H, E_H)$  is a subgraph of another graph  $G = (V, E)$  if  $V_H \subseteq V$  and  $E_H \subseteq E$ . Thus, let  $B$  be a matrix of  $i \times j$  with entries  $b_{ij} \in (D_i)_j$  when  $j \in \{1, \dots, 5\}$ . The matrix  $A$  is obtained with entries  $a_{ij} = b_{ij}$  if  $b_{ij} > 0$ , and  $a_{ij} = 0$  if  $b_{ij} \leq 0$ .

We computed the Euclidean distance between elements in each row in the matrix  $A$ , which produces a sequence of symmetric matrices  $W_i$ . Let  $m_i$  be the average of the row  $i$  of matrix  $A$ . Then, we build a sequence of graphs  $G_i$  for each matrix  $W_i$ , such that there is an edge between vertex  $u$  and vertex  $v$  if  $(w_i)_{uv} < m_i$ . We compare the distance between two sites for each year, assigning an edge for differences smaller than the averages. The existence of an edge represents similar WE variations between two sites.

The density and largest clique of each graph were calculated to understand the WE structure and spread. We recall that the density of a graph  $G$  is

$$\text{den}(G) = \frac{m}{n(n-1)/2} \quad (3)$$

where the graph density is the proportion between the number of existing edges and the total possible edges, i.e., the higher the density, the higher the WE spread over the whole metropolitan area. The largest clique is the complete subgraph with the largest number of nodes, representing the number of sites that exhibited similar values in the WE magnitude. We recall that a complete graph is produced when every vertex is joined to all other vertex by edges.

### 2.5. Statistical Analyses

The SIMAT, SIMAJ, and SIMA air pollutant data sets were analysed extensively using the *openair* package v2.1-5 [33] for R software v3.1.2 [34]. Peak probability distributions were computed using Python 2.7 with Pandas 0.20.3, numpy 1.13.3, and Matplotlib 2.1.1 packages. Long-term changes in the WE were computed with the TheilSen function included in *openair*, which allows testing the presence of a statistically significant monotonic linear trend. TheilSen relies on the non-parametric Mann-Kendall test to estimate the linear trend slope and intercept, which is quantified with the non-parametric Sen's test. Further details can be found elsewhere [21]. Statistical analyses were performed with the computational software SPSS 25.0 for Microsoft Windows.

## 3. Results

### 3.1. The WE Occurrence

The three MAs studied here have particular tropospheric photochemical environments associated to differences in local precursor emissions sources and meteorology [24,35,36]. Overall, the WE occurrence in ground-level  $O_3$  has been defined in Equation (1) as the existence of higher daytime averages (06:00–18:00 CDT) for Sat–Sun than for Tue–Thu [12,31]. Figure 3 shows that all MAs studied here experience the WE occurrence in all years in at least one monitoring site. Higher  $O_3$  levels on weekends arise from reduced  $O_3$  titration due to lower  $NO_x$  emissions mostly from diesel powered vehicles than during weekdays [37]. Hernández-Paniagua et al. reported significant decreases in  $NO_x$  levels for these three MAs during weekends, which explains the WE occurrence incidence [21]. For most of the years, the GMA and MMA show a WE occurrence in >40% of each year weeks, while since 2002 the largest occurrences are observed clearly at the MMA with no apparent trend. By contrast, the MCMA and GMA exhibit large variation in the WE occurrence between 2000 and 2012, and a marked increase since 2013 and 2012, respectively. A comparison made since 1996 when there are data available for all MAs reveals the existence of significant differences ( $p < 0.05$ ) in the WE occurrence among MAs. Furthermore, the later WE increase at the GMA and MCMA is opposite to the apparent decrease observed since 2013 for the MMA, which suggests significant variations across MAs of Mexico.

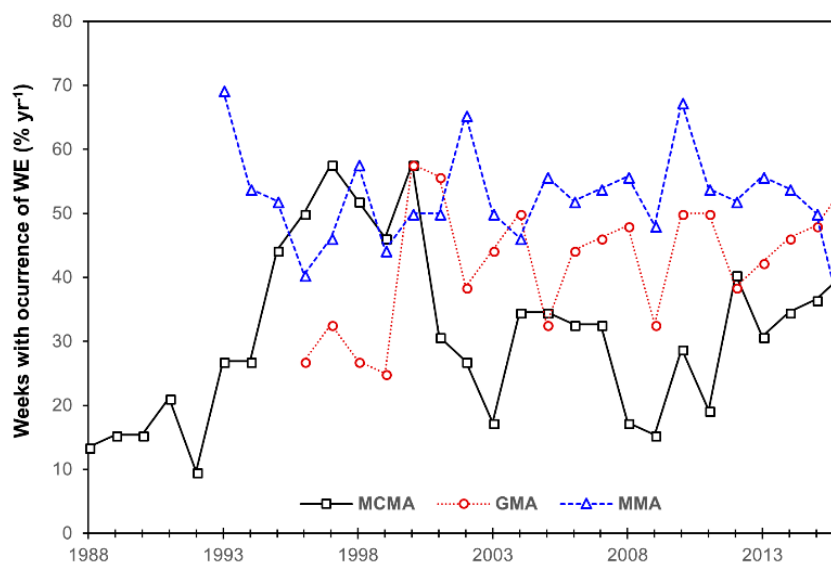


**Figure 3.** Percentage of weeks by year with weekend effect (WE) occurrence within the MCMA, GMA, and MMA. The WE occur whether at least one of the sites in each metropolitan area (MA) exhibits higher Sat–Sun daytime  $O_3$  averages (06:00–18:00 CDT) than Tue–Thu daytime averages.

### 3.2. Weekend/Weekday Differences in the $O_3$ Peaks

An additional method in ground-level  $O_3$  peaks (1 h averages) for observed differences on Wednesday, Saturday, and Sunday, defined as reference days, was used to test the WE occurrence as shown in Equation (2).  $O_3$  peaks may be higher on weekends than during weekdays despite lower levels in traffic and  $O_3$  precursor [38]. Therefore, the WE occurrence and magnitude may exhibit variations from city to city. The weekend-to-weekday difference variations may provide insights of changes in  $O_3$  precursor emission dynamics over time in response to the introduction of air quality control strategies. Table 1 summarizes the minimum, average (mean), and maximum  $O_3$  peak differences for each MA. It should be noted that negative differences correspond to higher  $O_3$  peaks during weekdays than during weekends (no WE occurrence), while positive differences correspond to higher  $O_3$  peaks during weekends (WE occurrence). Within the MCMA, the largest differences for the no WE occurrence were observed all at PED in 1992 for Sat/Wed (−234 ppb  $O_3$ ), in 1992 for Sun/Wed (−235 ppb  $O_3$ ) and in 1992 for Sat–Sun/Tue–Thu (−106 ppb  $O_3$ ). By contrast, the largest WE occurrence was observed at PED for Sat/Wed in 1988 (205 ppb  $O_3$ ) and Sat–Sun/Tue–Thu in 1997 (65 ppb  $O_3$ ), and at MER in 1992 for Sun/Wed (180 ppb  $O_3$ ).

For the GMA, higher  $O_3$  peaks on weekdays than on weekends were observed at VAL for Sat/Wed in 1996 (−190 ppb  $O_3$ ) and for Sun/Wed in 1996 (−169 ppb  $O_3$ ), while MIR showed the largest for Sat–Sun/Tue–Thu in 1997 (−59 ppb  $O_3$ ). The largest WE occurrence within the GMA was observed at CEN for Sat/Wed in 1997 (169 ppb  $O_3$ ), at VAL for Sun/Wed in 1997 (143 ppb  $O_3$ ), and at TLA for Sat–Sun/Tue–Thu in 2010 (58 ppb  $O_3$ ). Higher  $O_3$  peaks during weekdays lead to no WE occurrence regularly at STA, with the largest differences observed for Wed/Sat in 1993 (−116 ppb  $O_3$ ) and Wed/Sun in 1993 (−143 ppb  $O_3$ ). For Sat–Sun/Tue–Thu, the largest difference was observed at SNB in 2004 (−47 ppb  $O_3$ ). The largest magnitude in the WE occurrence was observed at STA for Wed/Sat (125 ppb  $O_3$ ) and Wed/Sun (138 ppb  $O_3$ ) in 1994 and 2004, respectively, and at OBI for Sat–Sun/Tue–Thu in 2004 (52 ppb  $O_3$ ). Among the three MAs, the MMA exhibited the lowest differences for the occurrence and no WE occurrence, despite showing the largest number of weeks per year with WE occurrence. These differences suggest that  $O_3$  levels change moderately from weekdays to weekends compared to the MCMA and GMA.

**Table 1.** Descriptive statistics for the weekend/weekday differences in O<sub>3</sub> peaks and daytime averages. Max values correspond to the magnitude of the WE occurrence.

Metropolitan Area	Site	Sat/Wed			Sun/Wed			Sat–Sun/Tue–Thu		
		Min	Average	Max	Min	Average	Max	Min	Average	Max
MCMA 1986–2016	MER	−188	3	186	−191	−2	180	−73	1	46
	PED	−234	1	205	−235	−10	176	−106	0	65
	SAG	−118	2	123	−156	0	133	−44	1	45
	TLA	−232	2	190	−213	−1	148	−53	1	51
	XAL	−192	3	140	−154	3	164	−48	2	52
GMA 1996–2016	ATE	−129	0	131	−114	−4	116	−56	0	56
	CEN	−143	3	169	−166	−3	106	−46	1	54
	MIR	−145	1	125	−145	−2	105	−59	0	57
	TLA	−120	2	157	−145	−2	114	−53	1	58
	VAL	−190	1	144	−169	−4	143	−46	1	54
MMA 1993–2016	GPE	−106	−1	88	−134	−2	102	−45	0	44
	SNN	−100	−1	86	−104	−2	89	−34	0	34
	OBI	−115	0	102	−136	0	133	−45	2	52
	SNB	−104	−1	113	−109	−2	84	−47	0	45
	STA	−116	−1	125	−143	−3	138	−41	1	45

It is clear that the largest weekday/weekend differences are observed at sites downwind and close to highly trafficked roads in all MAs. This is consistent with enhanced O<sub>3</sub> titration by abundant vehicular emissions during weekdays but reduced during weekends [39]. Such behaviour can be explained by the urbanization degree as proposed by Atkinson-Palombo et al. [31], which suggests that changes in the O<sub>3</sub> WE are a function of traffic count, population, and employment within 4 km zones around each site. Although O<sub>3</sub> measurements started in different year, most of the largest variations are observed by the beginning of the monitoring at the three MAs. It can be interpreted to indicate large weekday/weekend changes in emissions from motor vehicles during the 1990s prior to the mandatory three-way catalytic converter introduction for all vehicles in 1993 in the country [18]. Furthermore, the O<sub>3</sub> WE magnitude is proportional to the O<sub>3</sub> and NO<sub>x</sub> levels observed at each MA, which explains the largest differences in the WE observed for the MCMA, where air pollutants levels are typically higher than in the GMA and MMA [20,21,40].

### 3.3. Long-Term Trends in the WE

Quantifying the absolute change in the overall O<sub>3</sub> levels and WE magnitude is crucial to evaluate the success of air quality policies introduced for controlling precursor emissions. The secular trends in O<sub>3</sub> peaks differences and daytime averages were calculated from annual averages, derived from monthly averages, which were filtered with the STL technique to discard meteorological influences on the calculated trends [41]. Although no significant differences ( $p > 0.05$ ) were observed between filtered and non-filtered annual averages for all cities, filtered data were used for the trends calculation as reported elsewhere [21,42]. Figure 4 shows the linear fittings for the O<sub>3</sub> differences at all sites and MAs, and Table 2 lists the parameterisation of the trends. Overall, only the MCMA exhibits significant increasing trends ( $p < 0.1$ ) for all sites in the Sun/Wed difference, while only PED shows significant increases for all metrics. Although all sites within the MCMA exhibit year-to-year variations, the range of these decreases over time and shifts to WE occurrence as noted clearly for Sun/Wed (Figure 4). The trend linearization of differences with the Mann–Kendall approach shows increasing rates for Sun/Wed ranging from 0.33 ppb O<sub>3</sub> yr<sup>−1</sup> (0.03% yr<sup>−1</sup>) at SAG to 1.29 ppb O<sub>3</sub> yr<sup>−1</sup> (0.13% yr<sup>−1</sup>) at PED. The WE increases at PED for Sat/Wed and Sat–Sun/Tue–Thu correspond to growth rates of 0.42 and 038 ppb yr<sup>−1</sup> (0.04 and 0.04% yr<sup>−1</sup>), respectively. Such trends suggest that the magnitude of the O<sub>3</sub> WE will continue to increase within the whole MCMA and more strongly at downwind sites.

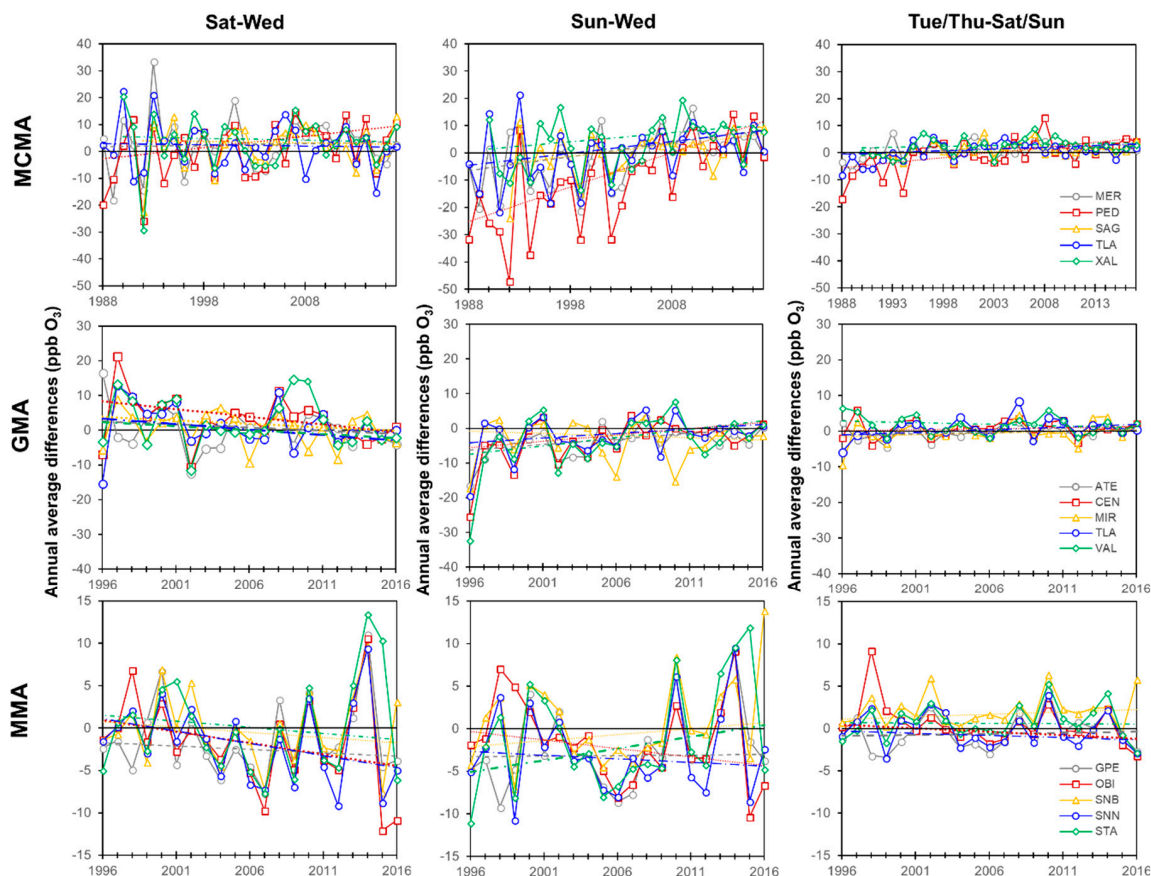


**Figure 4.** Long-term trends for O<sub>3</sub> peaks and daytime averages of reference days within the MCMA during 1988–2016, GMA during 1996–2016, and MMA during 1993–2016. Each data point represents the annual average that defines the year. The continuous lines show the Sen trend.

**Table 2.** Summary of rates of change in the O<sub>3</sub> WE magnitude at the three metropolitan areas.

Metropolitan Area	Site	Rates of Change								
		Sat/Wed			Sun/Wed			Sat–Sun/Tue–Thu		
		ppb yr <sup>−1</sup>	% yr <sup>−1</sup>	<i>p</i>	ppb yr <sup>−1</sup>	% yr <sup>−1</sup>	<i>p</i>	ppb yr <sup>−1</sup>	% yr <sup>−1</sup>	<i>p</i>
MCMA	MER	0.08	0.01		0.64	0.06	***	0.11	0.01	
	PED	0.42	0.04	*	1.29	0.13	***	0.38	0.04	***
	SAG	−0.05	−0.01		0.42	0.04	+	0.08	0.01	
	TLA	−0.05	0.02		0.34	0.04	*	0.09	0.01	
	XAL	−0.07	−0.01		0.33	0.03	*	0.07	0.01	
GMA	ATE	−0.15	−0.02		0.32	0.03	+	0.07	0.01	
	CEN	−0.44	−0.04		0.41	0.04	+	0.05	0.01	
	MIR	−0.16	−0.02		−0.08	−0.01		0.10	0.01	
	TLA	−0.37	−0.03		0.26	0.03		0.05	0.01	
	VAL	−0.23	−0.02		0.48	0.05	*	−0.09	−0.01	
MMA	GPE	−0.08	−0.01		0.00	0.00		0.02	0.00	
	SNN	−0.17	−0.03	+	−0.11	−0.02		−0.08	0.01	
	OBI	−0.12	−0.01		0.10	0.01		0.02	0.01	
	SNB	−0.16	−0.03		−0.08	−0.01		−0.04	−0.01	
	STA	−0.05	−0.01		0.33	0.03		0.00	0.00	

+ Level of significance *p* < 0.1. \* Level of significance *p* < 0.05. \*\*\* Level of significance *p* < 0.001.

The MCMA WE trends are compared with those calculated for the GMA and MMA to discuss them in a national context. Only the GMA exhibits significant increases (*p* < 0.1) in the WE magnitude for the Sun/Wed differences at ATE (0.32 ppb O<sub>3</sub> yr<sup>−1</sup>; 0.03% yr<sup>−1</sup>), CEN (0.41 ppb O<sub>3</sub> yr<sup>−1</sup>; 0.04% yr<sup>−1</sup>), and VAL (0.48 ppb O<sub>3</sub> yr<sup>−1</sup>; 0.05% yr<sup>−1</sup>). By contrast, the MMA shows no increasing trends for O<sub>3</sub> levels on weekends for all sites. Furthermore, the SNN upwind site exhibits a significant decrease in

the Sat/Wed differences of  $0.17 \text{ ppb O}_3 \text{ yr}^{-1}$  in response to larger  $\text{O}_3$  levels during weekdays. This is consistent with persistent increases in  $\text{NO}_x$  and the higher increase in  $\text{O}_3$  levels reported for SNN compared to other sites within the MMA [20]. Although apparent but no significant ( $p > 0.1$ ) decreases for the Sat/Wed differences are noticeable within the GMA and MMA, year-to-year variations could influence the trends significance. Furthermore, opposite trends for the Sun/Wed differences between the GMA and MMA suggest different emission scenarios for them. Nevertheless, STA and OBI at the MMA that show no significant increases for the WE Sun/Wed during 1993–2016 may become significant in future years resembling the behaviour observed currently within MCMA.

### 3.4. Compliance with the Mexican Official Standards for $\text{O}_3$

To standardize the exceedances number per year during weekends, the 95 ppb  $\text{O}_3$  latest standard was used to determine how the compliance with the official standard has changed over time at the three MAs. Figure 5 shows that at all MAs the  $\text{O}_3$  1 h official standard was exceeded both on Saturdays and Sundays in all years in at least one monitoring site [40]. Within the MCMA, the largest number of exceedances is seen at the downwind PED site, which is consistent with the largest observed exceedances number in the MMA at the downwind STA site, while in the GMA no clear pattern is observed. The breaches number to the  $\text{O}_3$  1 h official standard have decreased markedly within the MCMA since the 1990s, while no apparent trends are observed for the GMA and MMA. Nevertheless, there have been years with severe increases in the breaches number within the GMA at all sites, for instance between 2010 and 2011, and within the MMA in 2005 and 2014. By contrast, within the MCMA, only PED exhibits an increase in the breaches number more noticeable on Sundays since 2014. The increase in the annual breaches number to the  $\text{O}_3$  official standard is explained by the WE increasing magnitude observed at PED.

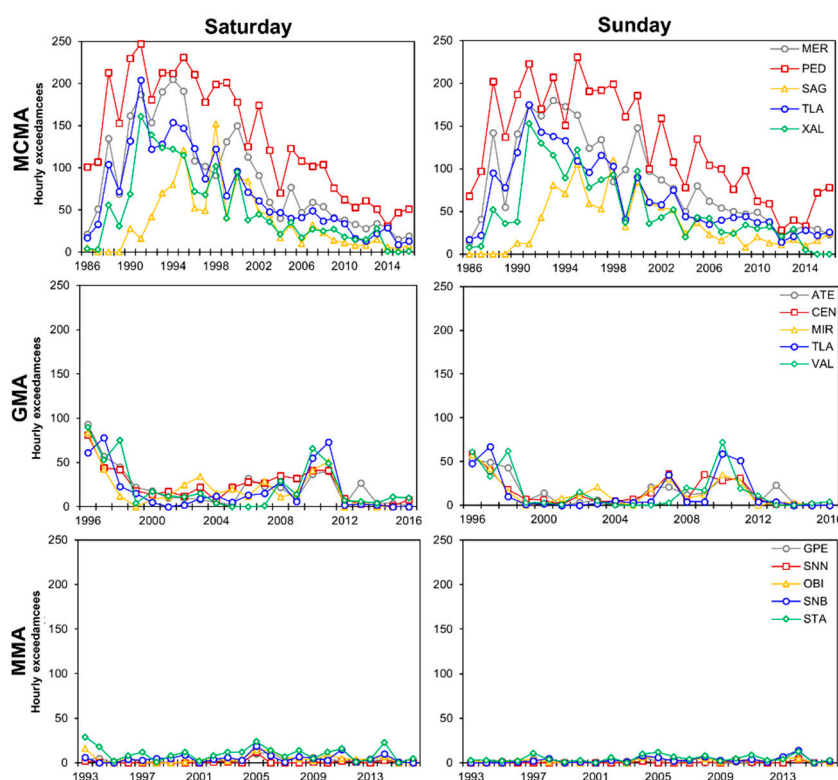


Figure 5. Number of exceedances per year to the  $\text{O}_3$  1 h average Mexican official standard of 95 ppb.

## 4. Discussion and Conclusions

Air pollutants record levels observed within the MCMA between the late 1980s and early 1990s led to the introduction of numerous strategies to improve the air quality [18]. The strategies to control  $\text{O}_3$

precursor emissions have been effective notably within the MCMA, as annual averages of ground-level O<sub>3</sub> represent around 50% of those observed in the early 1990s [29]. While there have been significant efforts to control the air pollutants levels within the MCMA, the GMA, and MMA have received less attention from the environmental authorities because the typical pollutant levels are lower than within the MCMA [26]. Nevertheless, the three MAs experience frequently recurrent breaches to the 1 h O<sub>3</sub> official standard [21]. Indeed, the moderate increase in O<sub>3</sub> levels within the MCMA observed since 2013 and markedly in 2016 has resulted in further increases to the breaches number to the O<sub>3</sub> official standard at some sites (Figure 5) [22]. Within the GMA and MMA, O<sub>3</sub> long-term trends differ from those observed in the MCMA [21]. This highlights the specific strategies need to control O<sub>3</sub> levels for each MA, which consider the local air quality scenarios and precursor emissions sources.

#### 4.1. Changes in the O<sub>3</sub> Precursor Emissions

Weekend/weekday differences in O<sub>3</sub> levels arise from reduced NO<sub>x</sub> emissions on weekends and vary in magnitude from city to city due to the particular chemical environments [38]. Although meteorology may influence the O<sub>3</sub> WE on short time scales [24], the variations occur during periods no longer than weeks and have no significant effects on O<sub>3</sub> WE long-term trends [12]. By contrast, long-term changes in the WE occurrence have been associated with the introduction of long-term programs for reducing O<sub>3</sub> precursor emissions [16]. In particular, the O<sub>3</sub> WE occurrence and spread have been ascribed to larger reduction in VOC emissions than in NO<sub>x</sub> emissions, which has resulted in environments where O<sub>3</sub> production is VOC-limited. For instance, in urban areas of California, Marr and Harley [13] reported the WE spread from few to many monitoring sites from 1980 to 1999 because national control strategies caused larger reductions in VOC emissions than in NO<sub>x</sub> emissions. By contrast, Wolff et al. reported the WE shift away in urban areas across the US from 35% to less than 5% of monitoring sites that exhibited WE in the late 1990s [12], because changes in control policies favoured larger declines in NO<sub>x</sub> than in VOC emissions.

In Mexico, the strategies to control O<sub>3</sub> levels have been directed to reduce emissions from industrial, commercial, and motor vehicle sources [18,29]. At national scale, the highest annual NO<sub>x</sub> emissions correspond to motor vehicles that contribute in around 46% of the total, while motor vehicles and commercial sources contribute similarly in around 16% and 20% of total annual VOC emissions, respectively [43]. While motor vehicles have represented a feasible opportunity to control NO<sub>x</sub> emissions, wider strategies have been required to reduce VOC emissions. A detailed description of all implemented air quality control policies in MAs of Mexico can be found elsewhere [18,21,28,44]. To clarify whether the increasing WE arises from lower decreases in NO<sub>x</sub> emissions during weekends compared with those during weekdays, we used ground-based measurements for reference days of NO<sub>x</sub> restricted to the 06:00–09:00 CDT period, when ambient levels are dominated by emissions from motor vehicles [45].

Figure 6 shows the long-term trends for reference days and overall ground-level NO<sub>x</sub>, and Table 3 lists the parameterization of the trends. Within the MCMA, the larger significant decreases ( $p < 0.05$ ) are observed for the overall data set at all sites, ranging from 0.2 to 1.1 ppb yr<sup>-1</sup> during 1988–2016, apart from SAG. Lower decreases in NO<sub>x</sub> are observed for the restricted rush hour period. Only on Sundays, all sites exhibit significant trends, with decreases at MER, PED, and XAL and increases at SAG and TLA. The MER and PED sites are predominantly influenced by local emissions both of petrol and diesel fuelled vehicles and aged air masses from the northern area of the MCMA, while SAG is an upwind site relatively away from the urban area with less vehicular influence.

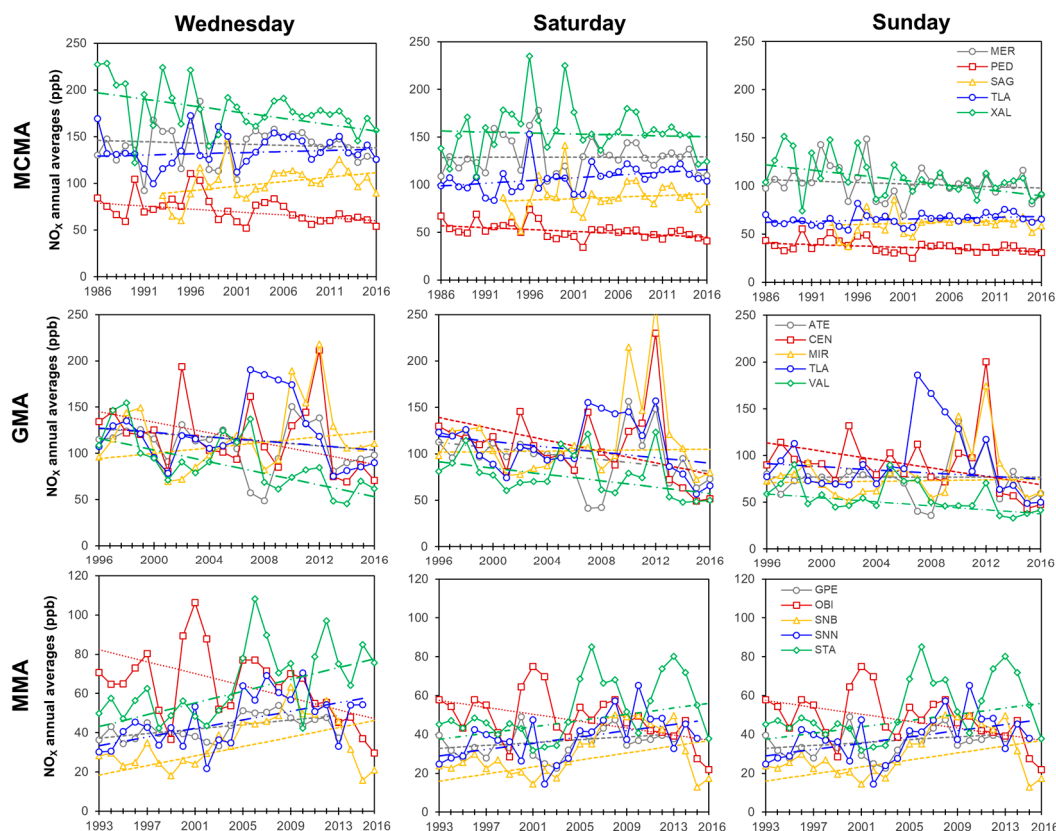


Figure 6. Long-term trends in  $\text{NO}_x$  annual averages calculated constrained to 06:00–09:00 CDT.

Table 3. Annual rates of change for  $\text{NO}_x$  long-term trend between 06:00–09:00 CDT expressed in  $\text{ppb yr}^{-1}$  during the studied periods within the three metropolitan areas.

Metropolitan Area	Site	Rates of Change											
		Wednesday			Saturday			Sunday			Overall		
		$\text{ppb yr}^{-1}$	$\% \text{ yr}^{-1}$	<i>p</i>	$\text{ppb yr}^{-1}$	$\% \text{ yr}^{-1}$	<i>p</i>	$\text{ppb yr}^{-1}$	$\% \text{ yr}^{-1}$	<i>p</i>	$\text{ppb yr}^{-1}$	$\% \text{ yr}^{-1}$	<i>p</i>
MCMA 1988–2016	MER	−0.1	−0.2		0.0	0.0		−0.3	−0.3	*	−1.0	−1.0	***
	PED	−0.6	−0.8	***	−0.4	−0.7	***	−0.3	−0.7	***	−1.0	−1.7	***
	SAG	1.0	1.1		0.3	0.4		0.4	0.4	**	0.0	0.0	
	TLA	0.3	0.2		0.6	0.6	***	0.2	0.3	*	−0.2	−0.3	*
	XAL	−1.3	0.7	***	−0.2	−0.1		−1.0	−0.9	***	−1.1	−1.1	***
GMA 1996–2016	ATE	−1.1	−0.9	+	−1.6	−1.4	*	0.0	0.0		−0.9	−1.4	
	CEN	−2.8	−2.0	*	−3.1	−2.2	*	−2.2	−2.0	*	−2.0	−2.1	*
	MIR	1.5	1.6	*	0.2	0.2		0.2	0.3		0.0	0.1	
	TLA	−1.2	−0.9		−1.5	−1.2		−0.8	−0.9		−1.0	−1.3	
MMA 1996–2016	VAL	−3.2	−2.7	***	−1.7	−1.9	*	−1.1	−1.8	***	−1.6	−2.6	***
	GPE	0.6	1.6	*	0.4	1.1	*	0.4	1.1	*	0.2	0.1	+
	SNN	1.1	3.3	**	0.8	2.9	**	0.8	2.8	*	0.4	1.8	***
	OBI	−1.5	−1.9	**	−0.9	−1.6	*	−0.9	−1.6	*	−0.9	−1.8	***
	SNB	1.2	6.6	+	0.9	5.6		0.9	5.6		0.5	3.4	
STA	1.5	3.5	**	0.8	2.2	+	0.8	2.2	+	0.3	0.8		

+ Level of significance  $p < 0.1$ . \* Level of significance  $p < 0.05$ . \*\* Level of significance  $p < 0.01$ . \*\*\* Level of significance  $p < 0.001$ .

For the GMA, only CEN and VAL exhibit significant decreases in the overall  $\text{NO}_x$ , while only VAL shows a significant decrease on all days. The VAL site is predominantly influenced by emissions from petrol and diesel vehicular activity, mostly from the Mexico and Avila Camacho avenues, which exhibit reduced diesel traffic on Sundays. By contrast, within the MMA, only OBI shows significant decreases on all days in marked contrast to the increases observed at the other sites. Indeed, both the industrials upwind SNN and the downwind STA sites show significant increases for all days during the restricted rush hour period. It is likely that industrial emissions could be offsetting the trends in vehicle emissions despite the period restriction imposed to the analysis. The decreases in  $\text{NO}_x$  determined at OBI are consistent with those observed at sites strongly influenced by vehicular emissions at the MCMA and

GMA. This provides evidence that policies implemented to reduce NO<sub>x</sub> emissions from motor vehicles have yielded significant results nationwide.

Accurate data of long-term changes in VOCs levels can help to unveil the origin for the WE magnitude increase observed at monitoring sites within the MCMA and GMA. Nevertheless, while the outlook for ground-level NO<sub>x</sub> is clear at the three MAs, no conclusive results have been reported for VOCs. This is partially due to the lack of continuous monitoring of VOCs because these are not criteria pollutants, neither considered in the current legislation. Furthermore, the scarce information of VOC levels over time within the MCMA have been obtained during short field campaigns, while the existing data for the GMA and MMA reported to date do not allow a trend comparison.

Overall, from measurements made at MER and PED for VOCs levels within the MCMA in 2012, Jaimes-Palomera et al. reported reductions in light alkane and aromatic levels during the morning rush hour compared to 2003 levels [46], which were consistent with the decrease in VOCs levels reported by Garzón et al. from 2002 to 2012 [47]. For the same sites, Arriaga-Colina et al. and Velasco et al. suggested an apparent stabilization/decrease in the total levels of around 50 species of VOCs [48,49]. Such studies suggest that strategies to control VOC emissions within the MCMA have been effective to some extent. However, in terms of VOCs level changes, the overall successful decrease in O<sub>3</sub> levels within the MCMA has been ascribed to increases in ambient reactive olefins concentrations derived from changes in petrol composition along with reductions in levels of highly reactive VOCs [46]. Unfortunately, the uncertainties in national and local emission inventories estimates for VOCs do not allow to perform a direct comparison with field data [21]. Although the continuous measurements of VOCs that started in 2012 within the MCMA could help to understand the increasing WE, these are not publicly available to date. Nevertheless, emission estimates of VOCs with lower uncertainties are required also for a better design of control strategies.

#### 4.2. Long-Term and Spatial Distribution of the WE Occurrence

We observed variations in O<sub>3</sub> WE occurrence intra-cities, which is more widespread within the MCMA. Overall, increases in the WE are observed at downwind and urban core sites within the MCMA and GMA. This is consistent with the study of Atkinson-Palombo et al. made at Maricopa, Arizona, where higher variations in the WE at urban core sites were observed, in contrast with fringe sites that exhibited almost no WE effect [31]. This also agrees with a study made in Ontario, Canada, by Huryn and Gough who reported that urbanized sites, typical of urban cores, experience the WE occurrence recurrently, while fringe and rural sited do not [39]. It is likely that a growth in urbanization parameters such as population and vehicle fleet may have been influencing the WE spread in some regions of MCMA and GMA [18,21,26,28,39]. By contrast, within the MMA, growing emissions from an expanding industrial area may have offset the effect of urbanization on changes in the WE occurrence.

The spread and increase in the WE magnitude within the MCMA are confirmed by the spatial interaction analysis, which is consistent with results from the long-term trends approach. Because the WE spread occurs only within the MCMA; results are presented only for it. Figure 7 shows three annual WE interaction graphs representative cases ( $G_6, G_{16}, G_{25}$ ), constructed following the methodology described in Section 2.4. We recall that the sub-index represents a number in the sequence of graphs; for example,  $G_6$  represents the plot for 1997. It is clear how the interaction among monitoring sites has become stronger over time, with few interactions among sites during the 1990s and all possible interactions in 2016. This can be clearly seen in Figure 8a, where the density of the graph increases with the WE spread over time. High densities are observed from 2007 onwards despite year-to-year variations. Simultaneous increases in the size of the largest clique confirm the increasing magnitude of the WE (Figure 8b).

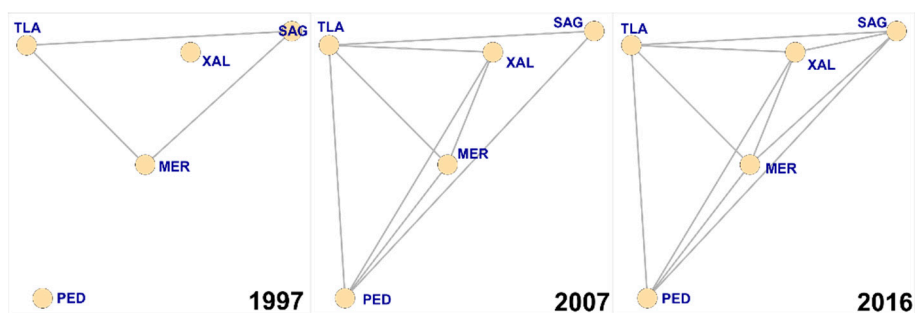


Figure 7. Representative cases of the WE effect spatial interaction among sites within the MCMA.

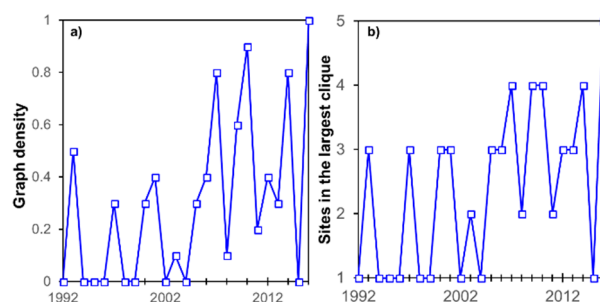


Figure 8. Graph measures over time. (a) Density for each graph; (b) Number of sites in the largest clique for each graph.

#### 4.3. Policy Implications

In this section, the successful strategies implemented to control ground-level  $O_3$  within the MCMA are presented and used to discuss the potential causes for the rise in the WE. We discuss also how higher levels in  $O_3$  during weekdays than during weekends within the GMA and MMA arise from the more stringent air quality control policies lack. Finally, the successful strategies that have helped to reduce the magnitude in the  $O_3$  WE implemented at MAs worldwide are presented.

Ground-level  $O_3$  decreased significantly within the MCMA during 1990–2016, remained with no significant changes within the GMA during 1996–2016, and increased within the MMA during 1993–2016 [21,22]. However, within the MCMA and GMA, we observed increases in the occurrence and magnitude of the WE that have led to increasing breaches to the 1 h  $O_3$  official standard during weekends after 2014 and 2008, respectively. Although control strategies have been effective in reducing  $O_3$  precursor emissions simultaneously, larger decreases in VOC emissions in the VOC-sensitive environments existing at the MCMA and GMA resulted in the spread and increase of the WE magnitude [36]. These increases are consistent with those reported in California during the 1990s in VOC-sensitive regions where large reductions in VOC emissions increased the WE in some regions [13]. By contrast, increasing  $O_3$  precursor emissions in the VOC-sensitivity environment at MMA have not significantly changed the WE occurrence [24,50]. It is likely that increasing emissions from the growing industrial activity within the MMA may control the WE effect spread. This behaviour was previously reported for the MCMA by Stephens et al., who observed similar or even higher  $O_3$  levels during weekdays between 1986 and 2008 when  $O_3$  precursor levels were much higher than they are currently [17]. Indeed, we show that at the MCMA, the WE is more noticeable from 2008 onwards after the period addressed by Stephens et al. [17].

Jaimes-Palomera et al. suggested that, although vehicles represent the VOC emissions major share within the MCMA [46], other sources are also significant and must be controlled to continue reducing  $O_3$  levels. It is clear also that the mandatory three-way catalytic converters introduction in new vehicles since 1993 have helped to reduce  $NO_x$  levels at the three MAs [51]. In particular, for the MCMA, the license-plate-based driving restriction, more stringent exhaust emissions inspection programs, and the public transport vehicle fleet replacement/update have been successful strategies

in reducing vehicle emissions [18]. While industrial emissions have only been reduced apparently at the MCMA and GMA, further strategies are required at the MMA to control O<sub>3</sub> levels.

Although the strategies implemented to date have controlled O<sub>3</sub> levels successfully, these have failed to control the WE within the MCMA and GMA. This has resulted in increases in the number of exceedances to the 1 h O<sub>3</sub> standard mostly during Sundays in such MAs. Furthermore, the WE spread and magnitude increase observed within the MCMA and GMA demonstrate the complexity of O<sub>3</sub> production and control. Finally, environmental authorities must consider that control strategies targeting NO<sub>x</sub> may result in higher O<sub>3</sub> levels in the short term due to the VOC-limited environments within the three MAs.

**Supplementary Materials:** The following are available online at <http://www.mdpi.com/2071-1050/10/9/3330/s1>, Table S1. Data capture of weekend and weekday O<sub>3</sub> 1-h averages during the time window defined from the peak probability distribution for all monitoring sites of the three metropolitan areas.

**Author Contributions:** I.Y.H.-P. designed the study, analysed the data, and drafted the manuscript. R.L.F. performed the exploratory data analysis, recovery, and validation. J.J.P.-M. compiled all applicable legislation. O.D.-R. downloaded the data and performed the statistical analyses. J.A.P.-C. calculated the spatial variations in the WE. A.F.-T. compiled statistics data and performed data analyses. L.G.R.-S. and A.G.-R. provided data and revised the manuscript. A.M. helped in the study design, revised the manuscript, and provided funding to perform the data analyses. All co-authors re-viewed, revised and approved the final manuscript.

**Funding:** This study received partial support from the Tecnológico de Monterrey through grant 002EICIR01.

**Acknowledgments:** Grateful acknowledgements are made to the Secretariat for the Environment of Mexico City, the Secretariat for the Environment and Territorial Development of the Jalisco State and the Secretariat for Sustainable Development of the Nuevo León State for the public domain records. The authors gratefully thank Manuel Ramírez for helping with the map work.

**Conflicts of Interest:** The authors declare no conflict of interest. The funding sponsors had no role in the design of the study; in the collection, analyses or interpretation of data; in the writing of the manuscript; nor in the decision to publish the results.

## References

1. Monks, P.S.; Archibald, A.T.; Colette, A.; Cooper, O.; Coyle, M.; Derwent, R.; Fowler, D.; Granier, C.; Law, K.S.; Mills, G.E.; et al. Tropospheric ozone and its precursors from the urban to the global scale from air quality to short-lived climate forcer. *Atmos. Chem. Phys.* **2015**, *15*, 8889–8973. [[CrossRef](#)]
2. Lelieveld, J.; Evans, J.S.; Fnais, M.; Giannadaki, D.; Pozzer, A. The contribution of outdoor air pollution sources to premature mortality on a global scale. *Nature* **2015**, *525*, 367. [[CrossRef](#)] [[PubMed](#)]
3. Stevenson, D.S.; Dentener, F.J.; Schultz, M.G.; Ellingsen, K.; Van Noije, T.P.C.; Wild, O.; Zeng, G.; Amann, M.; Atherton, C.S.; Bell, N.; et al. Multimodel ensemble simulations of present-day and near-future tropospheric ozone. *J. Geophys. Res.* **2006**, *111*, D08301. [[CrossRef](#)]
4. IPCC. *Climate Change 2013. The Physical Science Basis. Contribution of Working Group I to the Fifth Assessment Report of the Intergovernmental Panel on Climate Change*; Stocker, T.F., Qin, D., Plattner, G.-K., Tignor, M., Allen, S.K., Boschung, J., Nauels, A., Xia, Y., Bex, V., Midgley, P.M., Eds.; Cambridge University Press: Cambridge, UK; New York, NY, USA, 2013; 1535p.
5. Parrish, D.D.; Singh, H.B.; Molina, L.; Madronich, S. Air quality progress in North American megacities: A review. *Atmos. Environ.* **2011**, *45*, 7015–7025. [[CrossRef](#)]
6. Pusede, S.E.; Cohen, R.C. On the observed response of ozone to NO<sub>x</sub> and VOC reactivity reductions in San Joaquin Valley California 1995–present. *Atmos. Chem. Phys.* **2012**, *12*, 8323–8339. [[CrossRef](#)]
7. Pugliese, S.C.; Murphy, J.G.; Geddes, J.A.; Wang, J.M. The impacts of precursor reduction and meteorology on ground-level ozone in the Greater Toronto Area. *Atmos. Chem. Phys.* **2014**, *14*, 8197–8207. [[CrossRef](#)]
8. Jiménez, P.; Parra, R.; Gasso, S.; Baldasano, J.M. Modeling the ozone weekend effect in very complex terrains: A case study in the Northeastern Iberian Peninsula. *Atmos. Environ.* **2005**, *39*, 429–444. [[CrossRef](#)]
9. Cleveland, W.S.; Graedel, T.E.; Kleiner, B.; Warner, J.L. Sunday and workday variations in photochemical air pollutants in New Jersey and New York. *Science* **1974**, *186*, 1037–1038. [[CrossRef](#)] [[PubMed](#)]
10. Labron, F. A comparison of weekend and weekday ozone and hydrocarbon concentrations on the Baltimore-Washington Metropolitan Area. *Atmos. Environ.* **1975**, *9*, 861–863. [[CrossRef](#)]

11. Levitt, S.B.; Chock, D.P. Weekday–weekend pollutant studies of the Los Angeles Basin. *J. Air Pollut. Control Assoc.* **1976**, *26*, 1091–1092. [[CrossRef](#)]
12. Wolff, G.T.; Kahlbaum, D.F.; Heuss, J.M. The vanishing ozone weekday /weekend effect. *J. Air Waste Manag. Assoc.* **2013**, *63*, 292–299. [[CrossRef](#)] [[PubMed](#)]
13. Marr, L.C.; Harley, R.A. Spectral analysis of weekday–weekend differences in ambient ozone, nitrogen oxide, and non-methane hydrocarbon time series in California. *Atmos. Environ.* **2002**, *36*, 2327–2335. [[CrossRef](#)]
14. Riga-Karandinos, A.N.; Saitanis, C.; Arapis, G. Study of the weekday-weekend variation of air pollutants in a typical Mediterranean coastal town. *Int. J. Environ. Poll.* **2006**, *27*, 300–312. [[CrossRef](#)]
15. Tonse, S.R.; Brown, N.J.; Harley, R.A.; Jin, L. A process-analysis based study of the ozone weekend effect. *Atmos. Environ.* **2008**, *42*, 7728–7736. [[CrossRef](#)]
16. Seguel, R.J. Ozone weekend effect in Santiago, Chile. *Environ. Pollut.* **2012**, *162*, 72–79. [[CrossRef](#)] [[PubMed](#)]
17. Stephens, S.; Madronich, S.; Wu, F.; Olson, J.B.; Ramos, R.; Retama, A.; Muñoz, R. Weekly patterns of México City’s surface concentrations of CO, NO<sub>x</sub>, PM<sub>10</sub> and O<sub>3</sub> during 1986–2007. *Atmos. Chem. Phys.* **2008**, *8*, 5313–5325. [[CrossRef](#)]
18. ProAire-MCMA (Programa para Mejorar la Calidad del Aire de la Zona Metropolitana del Valle de México 2002–2010), Mexico City Local Government-State of Mexico Government. 2011. Available online: [http://www.aire.cdmx.gob.mx/descargas/publicaciones/flippingbook/proaire2011\\$-\\$2020/#p=1](http://www.aire.cdmx.gob.mx/descargas/publicaciones/flippingbook/proaire2011$-$2020/#p=1) (accessed on 28 August 2018).
19. Jaimes, P.M.; Bravo, A.H.; Sosa, E.R.; Cureño, G.I.; Retama, H.A.; Granados, G.G.; Becerra, A.E. Surface ozone concentration trends in Mexico City Metropolitan Area. In Proceedings of the Air and Waste Management Association’s Annual Conference and Exhibition AWMA, San Antonio, TX, USA, 19–22 June 2012; Volume 3, pp. 2273–2284.
20. Benítez-García, S.E.; Kanda, I.; Wakamatsu, S.; Okazaki, Y.; Kawano, M. Analysis of criteria air pollutant trends in three Mexican metropolitan areas. *Atmosphere* **2014**, *5*, 806–829. [[CrossRef](#)]
21. Hernández-Paniagua, I.Y.; Clemitshaw, K.C.; Mendoza, A. Observed trends in ground-level O<sub>3</sub> in Monterrey, México, during 1993–2014: Comparison with Mexico City and Guadalajara. *Atmos. Chem. Phys.* **2017**, *17*, 14. [[CrossRef](#)]
22. Velasco, E.; Retama, A. Ozone’s threat hits back Mexico city. *Sustain. Cities Soc.* **2017**, *31*, 260–263. [[CrossRef](#)]
23. García-Reynoso, A.; Jazcilevich, A.; Ruiz-Suarez, L.G.; Torres-Jardón, R.; Suárez Lastra, M.; Reséndiz Juárez, N.A. Ozone weekend effect analysis in México City. *Atmósfera* **2009**, *22*, 281–297.
24. Sierra, A.; Vanoye, A.Y.; Mendoza, A. Ozone sensitivity to its precursor emissions in northeastern Mexico for a summer air pollution episode. *J. Air Waste Manag.* **2013**, *63*, 1221–1233. [[CrossRef](#)]
25. INEGI (National Institute of Statistics and Geography): XIII Censo General de Población y Vivienda 2010, México. 2010. Available online: <http://www.censo2010.org.mx/> (accessed on 22 August 2018).
26. INE (Instituto Nacional de Ecología). *Cuarto Almanaque de datos y Tendencias de la Calidad del aire en 20 Ciudades Mexicanas 2000–2009*; INE-SEMARNAT: México City, Mexico, 2011; 405p.
27. SEDEMA (Secretaría del Medio Ambiente de la Ciudad de México). Inventario de Emisiones de la CDMX. Contaminantes Criterio, Tóxicos y de Efecto Invernadero. 2014. Available online: [http://www.aire.cdmx.gob.mx/descargas/publicaciones/flippingbook/inventario-emisiones-cdmx2014\\$-\\$2/IE-CDMX\\$-\\$2014.pdf](http://www.aire.cdmx.gob.mx/descargas/publicaciones/flippingbook/inventario-emisiones-cdmx2014$-$2/IE-CDMX$-$2014.pdf) (accessed on 8 August 2018).
28. ProAire-GDL (Programa para Mejorar la Calidad del Aire, Jalisco 2011–2020), SEMARNAT, Gobierno del estado de Jalisco. 2011. Available online: [https://www.gob.mx/cms/uploads/attachment/file/69282/13\\_ProAire\\_Jalisco.pdf](https://www.gob.mx/cms/uploads/attachment/file/69282/13_ProAire_Jalisco.pdf) (accessed on 24 August 2018).
29. SEDEMA (Secretaría del Medio Ambiente—G.D.F.). Estimación de las concentraciones de ozono con la simulación de 13 medidas de control de emisiones, incluidas en el PROAIRE 2002–2010. 2005. Available online: [http://www.aire.cdmx.gob.mx/descargas/publicaciones/gestion-ambiental-aire-memoria-documental\\$-\\$2001\\$-\\$2006/descargas/estimacion\\_ozono\\_proaire\\_dic2005.pdf](http://www.aire.cdmx.gob.mx/descargas/publicaciones/gestion-ambiental-aire-memoria-documental$-$2001$-$2006/descargas/estimacion_ozono_proaire_dic2005.pdf) (accessed on 10 August 2018).
30. Davis, L.W. Saturday driving restrictions fail to improve air quality in Mexico City. *Sci. Rep.* **2017**, *7*, 41652. [[CrossRef](#)] [[PubMed](#)]
31. Atkinson-Palombo, C.M.; Miller, J.A.; Balling, R.C., Jr. Quantifying the ozone “weekend effect” at various locations in Phoenix, Arizona. *Atmos. Environ.* **2006**, *40*, 7644–7658.

32. Diestel, R. *Graph Theory, Graduate Texts in Mathematics*, 5th ed.; Springer: Berlin/Heidelberg, German, 2017; ISBN 978-3-662-53621-6.
33. Carslaw, D.C.; Ropkins, K. Openair—An R package for air quality data analysis. *Environ. Model. Softw.* **2012**, *27–28*, 52–61. [[CrossRef](#)]
34. R Core Team. *R: A Language and Environment for Statistical Computing*; R Foundation for Statistical Computing: Vienna, Austria, 2013; ISBN 3-900051-07-0. Available online: [www.R-project.org](http://www.R-project.org) (accessed on 23 August 2018).
35. Torres-Jardon, R.; García-Reynoso, J.A.; Jazcilevich, A.; Ruiz-Suárez, L.G.; Keener, T.C. Assessment of the ozone-nitrogen oxide-volatile organic compound sensitivity of Mexico City through an indicator-based approach: Measurements and numerical simulations comparison. *J. Air Waste Manag. Assoc.* **2009**, *59*, 1155–1172. [[CrossRef](#)]
36. Kanda, I.; Basaldud, R.; Magaña, M.; Retama, A.; Kubo, R.; Wakamatsu, S. Comparison of ozone production regimes between two Mexican cities: Guadalajara and Mexico City. *Atmosphere* **2016**, *7*, 91. [[CrossRef](#)]
37. Gao, H.O.; Niemeier, D.A. The impact of rush hour traffic and mix on the ozone weekend effect in southern California. *Transp. Res. Transp. Environ.* **2007**, *12*, 83–98. [[CrossRef](#)]
38. Heuss, J.M.; Kahlbaum, D.F.; Wolff, G.T. Weekday/weekend ozone differences: What can we learn from them? *J. Air Waste Manag. Assoc.* **2003**, *53*, 772–788. [[CrossRef](#)]
39. Huryn, S.M.; Gough, W.A. Impact of urbanization on the ozone weekday/weekend effect in Southern Ontario, Canada. *Urban Clim.* **2014**, *8*, 11–20. [[CrossRef](#)]
40. SEMARNAT (Secretaría del Medio Ambiente y Recursos Naturales). Informe Nacional de Calidad del aire 2014. 2015. Available online: <http://sinaica.inecc.gob.mx/archivo/informes/Informe2014.pdf> (accessed on 20 August 2018).
41. Cleveland, R.B.; Cleveland, W.S.; McRae, J.; Terpenning, I. STL: A seasonal-trend decomposition procedure based on Loess. *J. Off. Stat.* **1990**, *6*, 3–33.
42. Salmi, T.; Määttä, A.; Anttila, P.; Ruoho-Airola, T.; Amnell, T. *Detecting Trends of Annual Values of Atmospheric Pollutants by the Mann–Kendall Test and Sen’s Slope Estimates—the Excel Template Application MAKESENS*; Publications on Air Quality Report code FMI-AQ–31; Finnish Meteorological Institute: Helsinki, Finland, 2002; Volume 31, pp. 1–35.
43. SEMARNAT (Secretaría del Medio Ambiente y Recursos Naturales). Inventario Nacional de Emisiones 2008, México, D.F. 2014. Available online: <http://sinea.semarnat.gob.mx/sinae.php?steprep=5&process=UkVQT1JURUFET1I=&r=NC4gRnVlbnRlIHkgRW50aWRhZGVzIEZlZGVyYXRpdmFzIDFwMDgu> (accessed on 5 August 2018).
44. ProAire-MMA (Programa de Gestión para Mejorar la Calidad del Aire del Estado de Nuevo León 2016–2025), SEMARNAT, Gobierno del Estado de Nuevo León. 2016. Available online: [https://www.gob.mx/cms/uploads/attachment/file/250974/ProAire\\_Nuevo\\_Leon.pdf](https://www.gob.mx/cms/uploads/attachment/file/250974/ProAire_Nuevo_Leon.pdf) (accessed on 24 August 2018).
45. Parrish, D.D. Critical evaluation of US on-road vehicle emission inventories. *Atmos. Environ.* **2006**, *40*, 2288–2300. [[CrossRef](#)]
46. Jaimes-Palomera, M.; Retama, A.; Elias-Castro, G.; Neria-Hernández, A.; Rivera-Hernández, O.; Velasco, E. Nonmethane hydrocarbons in the atmosphere of Mexico City: Results of the 2012 ozone-season campaign. *Atmos. Environ.* **2016**, *132*, 258–275. [[CrossRef](#)]
47. Garzón, J.P.; Huertas, J.L.; Magaña, M.; Huertas, M.E.; Cárdenas, B.; Watanabe, T.; Maeda, T.; Wakamatsu, S.; Blanco, S. Volatile organic compounds in the atmosphere of Mexico City. *Atmos. Environ.* **2015**, *119*, 415–429. [[CrossRef](#)]
48. Arriaga-Colina, J.L.; West, J.J.; Sosa, G.; Escalona, S.S.; Ordunez, R.M.; Cervantes, A.D.M. Measurements of VOCs in Mexico City (1992–2001) and evaluation of VOCs and CO in the emissions inventory. *Atmos. Environ.* **2004**, *38*, 2523–2533. [[CrossRef](#)]
49. Velasco, E.; Lamb, B.; Westberg, H.; Allwine, E.; Sosa, G.; Arriaga-Colina, J.L.; Jobson, B.T.; Alexander, M.L.; Prazeller, P.; Knighton, W.B.; et al. Distribution, magnitudes, reactivities, ratios and diurnal patterns of volatile organic compounds in the Valley of Mexico during the MCMA 2002 & 2003 field campaigns. *Atmos. Chem. Phys.* **2007**, *7*, 329–353.

50. Carrillo-Torres, E.R.; Hernández-Paniagua, I.Y.; Mendoza, A. Use of combined observational-and model derived photochemical indicators to assess the O<sub>3</sub>-NO<sub>x</sub>-VOC system sensitivity in urban areas. *Atmosphere* **2017**, *8*, 22. [[CrossRef](#)]
51. SEMARNAT (Secretaria del Medio Ambiente y Recursos Naturales). NOM–042 (Norma Oficial Mexicana NOM-042-ECOL-1993, que establece los límites máximos permisibles de emisión de hidrocarburos no quemados, monóxido de carbono, óxidos de nitrógeno y partículas suspendidas provenientes del escape de vehículos automotores nuevos en planta, así como de hidrocarburos evaporativos provenientes del sistema de combustible que usan gasolina, gas licuado de petróleo, gas natural y diésel de los mismos, con peso bruto vehicular que no exceda los 3856 kilogramos). *Diario Oficial de la Federación*, 22 October 1993.



© 2018 by the authors. Licensee MDPI, Basel, Switzerland. This article is an open access article distributed under the terms and conditions of the Creative Commons Attribution (CC BY) license (<http://creativecommons.org/licenses/by/4.0/>).